Tuning the Properties of Copper(II) Complexes with Tetra- and Pentadentate Bispidine (= 3,7-Diazabicyclo[3.3.1]nonane) Ligands

by **Peter Comba***, **Carlos Lopez de Laorden**, and **Hans Pritzkow**

Universität Heidelberg, Anorganisch-Chemisches Institut, Im Neuenheimer Feld 270, D-69120 Heidelberg (fax: +49-6221-54 66 17; e-mail: peter.comba@aci.uni-heidelberg.de)

Dedicated to Professor *André E. Merbach* on the occasion of his 65th birthday

The synthesis of a series of tetra- and pentadentate bispidine-type ligands (bispidine = 3,7-diazabicyclo[3.3.1]nonane) – tetradentate ligands are donor-substituted at C(2) and C(4), pentadentate ligands have an additional donor at N(3) or N(7), with pyridine, 2-methylpyridine, or quinoline donor moieties – and of their Cu^{II} complexes are reported, together with single-crystal structural analyses and solution studies (electrochemistry, electronic and EPR spectroscopy). Depending on the ligand geometry and on the co-ligands (solvent or counter anion), there are various structural forms (pseudo-*Jahn – Teller* elongation along all three molecular axes), and the structural data are correlated with the spectroscopic and electrochemical parameters.

Introduction. – The transition-metal-ion coordination chemistry of bispidine-type ligands (bispidine = 3,7-diazabicyclo[3.3.1]nonane; see **L1** – **L12** for ligand structures discussed in this publication) has attracted some attention due to the salient structural properties [1 – 3], high complex stabilities and uncommon metal-ion selectivities [4] and, in particular, because of their interesting reactivities [5 – 9], specifically with respect to efficient [10] and tuneable [7][8] substrate binding and activation. An important feature is that bispidine molecules are generally easy to prepare, and they are obtained in high yield [11 – 14], and that mono- as well as dinucleating ligands with various donor sets in well-defined and rigid geometries may be prepared (bi-, tetra-, penta-, and hexadentate ligands, preorganized for planar, square-pyramidal and *cis*-octahedral coordination geometries) [15 – 20].

Due to the rigidity of the adamantane-derived bispidine backbone and the elasticity of the coordination geometry, interesting types of structural variations have been observed [1 – 3][21][22]. In particular, for penta- and hexacoordinate Cu^{II} complexes, it was possible to isolate and structurally characterize – in dependence of *i*) the *ortho*-substituent of the pyridine donors at C(2) and C(4) (H or Me) [7], *ii*) the substituent at N(7) [3][21], or *iii*) the co-ligands [22] – complexes with the tetragonal elongation (pseudo-*Jahn – Teller* axis) along any of the three molecular axes.

So far, the chance to vary the donor set by a variation of the aldehyde and amine components in the two *Mannich* condensation steps (see *Scheme*) has not been used extensively. We, therefore, report here the syntheses of six new tetra- and pentadentate bispidine ligands with 2-methylpyridine and quinoline donors, and the structural, electrochemical, and spectroscopic properties of their Cu^{II} complexes. The structural properties, specifically with respect to the mode of pseudo-*Jahn – Teller*-type distortion,

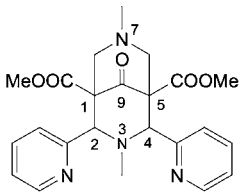

L1

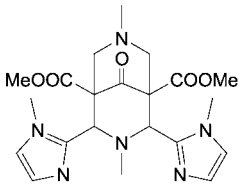

L2

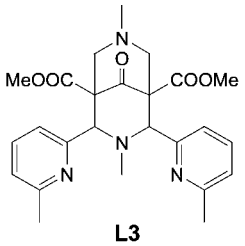

L3

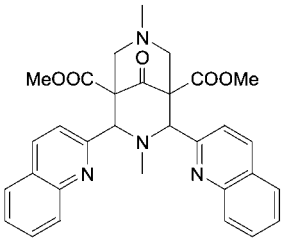

L4

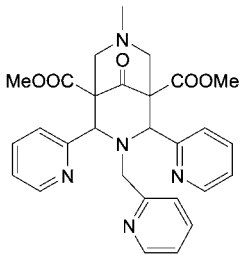

L5

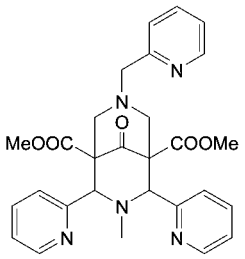

L6

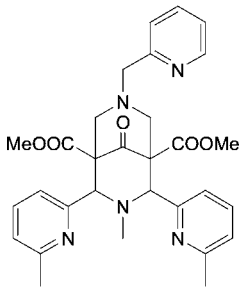

L7

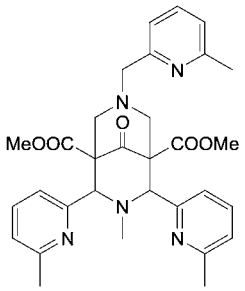

L8

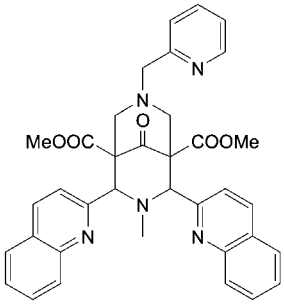

L9

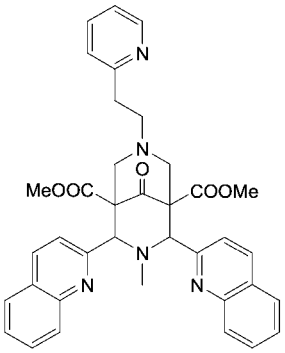

L10

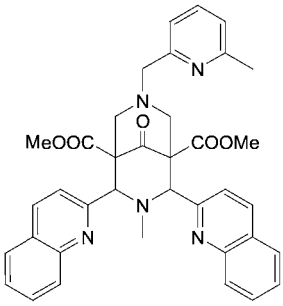

L11

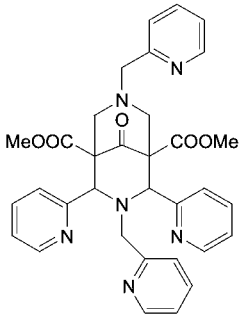

L12

Scheme

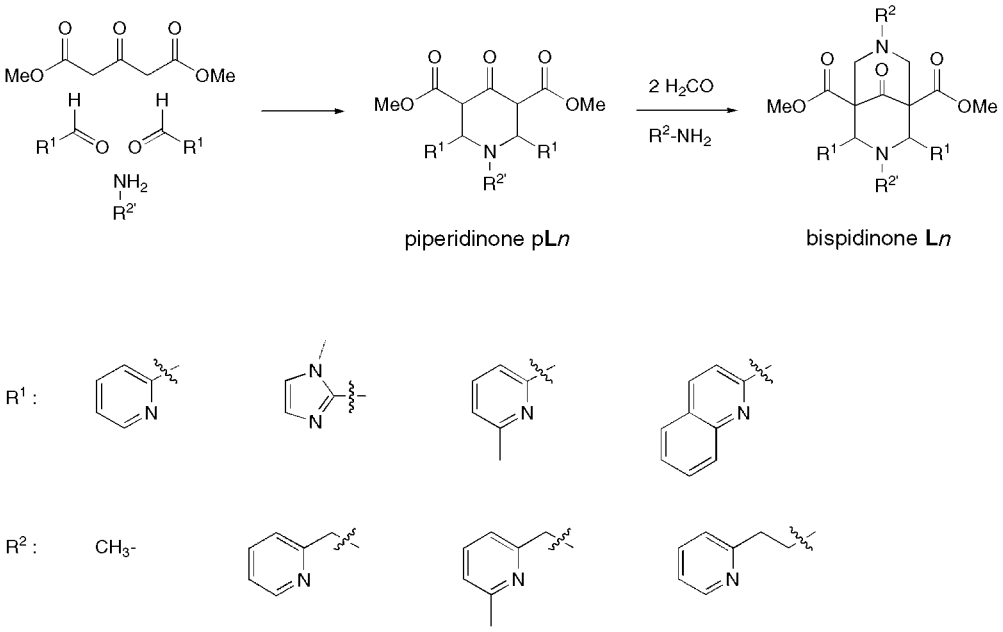

and the concomitant ligand-field properties and redox potentials are compared with those of the published systems with pyridine and 1*H*-imidazole donors, and discussed in detail.

Results and Discussion. – *Syntheses.* The ligands were prepared in analogy to the bispidinones described in the literature [4][7][11–14][20][23]; the two piperidinones and the six new bispidinones were obtained without difficulty and in respectable yields. A major possible impurity is the *exo-endo* form (orientation of the two donor substituents in 2,4-position); heating after the condensation which leads to the final product is necessary for isomerization to the thermodynamically more-stable, achiral *endo-endo* form [4][13][24][25]. Coordination to Cu^{II} or any other metal ion under strictly anhydrous conditions leads to the 9-keto form of the coordinated ligand (see structures of the chloro complexes with **L9** and **L11**; with water present, the hydrates at C(9) are formed as usual [3][4][21] (structures with **L4** and **L10**; with **L9**, isolated from MeOH, a C(9) methyl ether/alcohol-substituted product (MeO–C(9)–OH) is isolated, as observed for other complexes before [1]). Unfortunately, from the data for the complexes reported here, it is not possible to conclude unambiguously that the solution and solid-state data are obtained from structurally identical samples with respect to the C(9) substituents.

Solid-State Molecular Structures. The structures of the metal-free ligands **L8** and **L11** (see *Fig. 1*) are as expected, *i.e.*, similar to the ligand structure in the complexes,

with the exception that the three aromatic N-donors are rotated away from the center of the cavity due to lone-pair repulsion (low energy barrier) [4][23][26]. That is, the bispidine ligands are highly preorganized (and complementary for Cu^{II}) with respect to the tertiary amine moieties but not with respect to the aromatic N-donors.

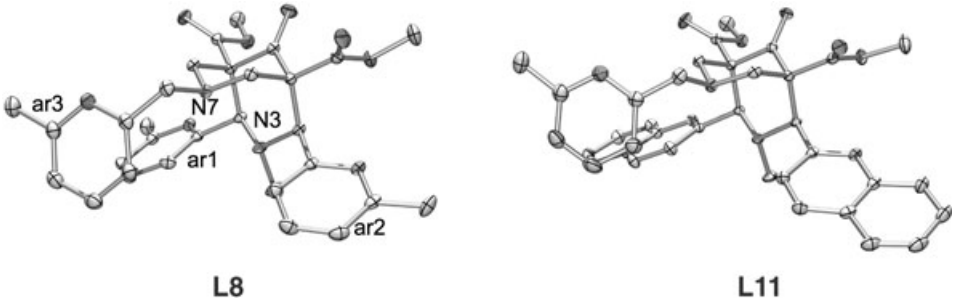

Fig. 1. *ORTEP*[36] *Plots of the metal-free bispidine ligands* **L3** *and* **L11**. Note that all aromatic N-donors are rotated away from the coordination site by *ca.* 180° due to lone-pair repulsion; IUPAC numbering (see *Table 1* for the crystallographic numbering).

As for transition-metal complexes with other tetra- [1], penta- [20], and hexadentate [4] bispidine ligands, the backbone of the bidentate fragment (bispidine = 3,7-diazabicyclo[3.3.1]nonane) is very rigid (see constant N(3) ··· N(7) distances in *Table 1*; for structural plots see *Fig. 2*; note that, in the discussion, we use the *IUPAC* numbering scheme given in Formula **L1**, which is different from the crystallographic numbering (see *Table 1*). The major variations in structures of [Cu^{II}(bispidine)] complexes in general are related to *i*) the torsional angles involving C(2) (or C(4)) and the corresponding C-atoms of the *trans*-disposed aromatic donors, *ii*) the orientation of the donors attached to N(3) or N(7) (chelate-ring conformation), and *iii*) the position of the metal ion in the bispidine cavity (see relative distances of the Cu^{II} center to N(3) and N(7) and the two *trans*-disposed donors at C(2) and C(4) (ar1 and ar2)), and, as a result of these distortions, the orientation of the '*Jahn–Teller* axis' in Cu^{II} complexes (see *Table 1*). The latter mode of distortion is of particular interest. With pentadentate ligands derived from **L5**, the Cu^{II} complexes with MeCN as the co-ligand exist in isomeric forms [21], one with an elongation along N(7)–Cu–N(ar3), the other with an elongated axis involving the two pyridine groups at C(2) and C(4) (N(ar1)–Cu–N(ar2)). A structural and spectroscopic analysis revealed that the two minima on the potential-energy surface (warped rim of the 'Mexican hat' potential-energy surface with three possible minima) were close to degenerate with the latter (elongation along the two *trans*-pyridines) being slightly more stable; sterically demanding substituents at N(7) or larger co-ligands such as Cl^- (see *Table 1*) lead to a destabilization of this isomer and a population of the other form [21] (more-recent structural and spectroscopic data confirm this conclusion [27]). With **L3** all three '*Jahn–Teller* isomers' were observed, *i.e.*, with Cl^- and OH_2 as co-ligands, there is an elongation along Cu–N(3), with MeCN along Cu–N(7), and with the bidentate ON O_2^- along N(ar1)–Cu–N(ar2) [22]. Two conclusions were obtained from these data of

Table 1. *Structural Data of [Cu(***Ln***)X]*$^{n+}$ [a])[b])

	[Cu(**L1**)Cl]$^{+}$[b])	[Cu(**L2**)Cl]$^{+}$[c])	[Cu(**L3**)Cl]$^{+}$[d])	[Cu(**L4**)Cl]$^{+}$[e])	[Cu(**L4**)F]$^{+}$	[Cu(**L5**)Cl]$^{+}$[c])	
Distances [Å]:							
Cu–N(1) (N(3))	2.042(3)	2.115(2)	*2.147(3)*	*2.149, 2.143(2)*	2.007(2)	2.070(2)	
Cu–N(2) (N(7))	*2.272(3)*	*2.316(2)*	2.120(3)	2.131, 2.135(2)	*2.254(2)*	*2.478(3)*	
Cu–N(3) (ar_1)	2.020(3)	1.967(2)	2.061(3)	2.001, 2.033(2)	2.087(2)	2.011(3)	
Cu–N(4) (ar_2)	2.024(3)	1.971(2)	2.064(3)	2.019, 2.017(2)	2.093(2)	1.987(3)	
Cu–N(5) (ar_3)	–	–	–	–	–	*2.544(3)*	
Cu–X	2.232(1)	2.229(1)	2.221(2)	2.265, 2.255(1)	1.836(2)	2.2545(1)	
N(1) ··· N(2)	2.921	2.917(2)	2.930(5)	2.922, 2.913(2)	2.902(2)	2.931(3)	
N(3) ··· N(4)	3.971	3.869(3)	4.084(5)	3.992, 4.016(2)	4.065(3)	3.965(4)	
Angles [°]:							
N(1)–Cu–N(2)	85.03(9)	82.20(6)	86.71(12)	86.11, 85.85(6)	85.67(7)	79.70(8)	
N(1)–Cu–N(3)	81.25(10)	80.58(7)	81.62(13)	82.80, 82.62(6)	80.39(8)	83.62(9)	
N(1)–Cu–N(4)	81.15(10)	80.51(7)	82.38(12)	82.92, 82.52(6)	80.05(8)	81.74(10)	
N(1)–Cu–N(5)	–	–	–	–	–	77.95(9)	
N(1)–Cu–X	165.02(7)	166.69(5)	112.97(9)	109.14, 109.88(4)	176.98(7)	173.81(7)	
N(2)–Cu–N(5)	–	–	–	–	155.11(8)		
N(3)–Cu–N(4)	158.13(10)	158.58(7)	163.82(13)	165.70, 165.04(6)	152.99(8)	165.36(10)	

	[Cu(**L6**)Cl]$^{+}$[c])	[Cu(**L9**)Cl]$^{+}$	[Cu(**L9**)OMe]$^{+}$	[Cu(**L10**)FBF_3]$^{+}$	[Cu(**L10**)]$^{2+}$	[Cu(**L11**)Cl]$^{+}$	[Cu(**L12**)]$^{2+}$[e])
Distances [Å]:							
Cu–N(1) (N(3))	2.036(2)	2.089(1)	2.042(4)	2.000(1)	1.953(2)	2.159(3)	2.087(3)
Cu–N(2) (N(7))	*2.368(2)*	2.114(2)	2.092(5)	2.169(1)	2.095(2)	2.079(3)	2.045(3)
Cu–N(3) (ar_1)	2.028(2)	*2.609(2)*	*2.374(4)*	*2.235(1)*	*2.311(2)*	*2.686(3)*	*2.280(3)*
Cu–N(4) (ar_2)	2.029(2)	*2.345(2)*	*2.523(4)*	*2.263(1)*	*2.269(2)*	*2.320(3)*	*2.798(4)*
Cu–N(5) (ar_3)	2.029(2)	2.019(2)	2.001(4)	1.984(1)	1.927(2)	2.159(3)	2.009(3)
Cu–X	*2.717(1)*	2.305(1)	2.058(4)	2.811(1)	–	2.264(1)	2.028(3)[h])
N(1) ··· N(2)	2.915(2)	2.853(2)	2.850(6)	2.876(1)	2.834(2)	2.836(4)	2.830(4)
N(3) ··· N(4)	3.995(3)	4.795(2)	4.746(6)	4.382(2)	4.464(3)	4.821(4)	4.672(4)
Angles [°]:							
N(1)–Cu–N(2)	82.53(6)	85.51(6)	87.14(16)	87.17(5)	88.80(7)	83.99(11)	86.43(12)
N(1)–Cu–N(3)	81.39(7)	74.68(5)	77.24(14)	80.39(5)	78.63(8)	73.06(10)	78.26(12)
N(1)–Cu–N(4)	80.94(7)	76.58(5)	75.59(14)	77.67(5)	80.07(8)	75.91(10)	72.98(11)
N(1)–Cu–N(5)	160.82(7)	164.80(6)	169.98(13)	174.53(6)	169.95(8)	160.09(11)	85.77(12)
N(1)–Cu–X	105.30(5)	97.35(4)	97.39(16)	89.12(5)	–	93.76(8)	154.39(13)
N(2)–Cu–N(5)	79.27(7)	83.29(6)	84.77(16)	97.02(6)	100.95(7)	83.46(11)	172.12(12)
N(3)–Cu–N(4)	160.07(7)	150.84(5)	151.50(13)	153.84(5)	154.18(7)	148.70(10)	148.53(10)

[a]) Atom numbering as in the crystal data; numbering in parenthases according to IUPAC rules (see *Formula* **L1**). [b]) Elongated bonds in italics. [c]) [19]. [d]) [7]. [e]) [23]. [f]) Two independent molecules in the unit cell. [g]) [4]. [h]) Cu–pyridine bond.

the (6-methylpyridin-2-yl)-substituted bispidine **L3**: *i*) the Me groups at the pyridine moieties destabilize the minimum with an elongated Cu–N(7) axis (co-ligand in-plane with the methylated pyridine donors, observed only for MeCN) and *ii*) the elongation along the two pyridine groups is the most favorable (but observed only with two co-ligands, *e.g.*, a chelating nitrate). This latter observation was emerging from solution spectroscopy and force-field, ligand-field, and DFT calculations [22] and was also confirmed by structural data of Cu^{II} complexes with the hexadentate ligand **L12** and a corresponding molecular-mechanical analysis [4].

The quinoline-based ligands **L4** (tetradentate), **L9**, **L10**, and **L11** (pentadentate) are, as the (6-methylpyridin-2-yl) based ligand **L3** and the corresponding new pentadentate ligands **L7** and **L8**, sterically more demanding than those with

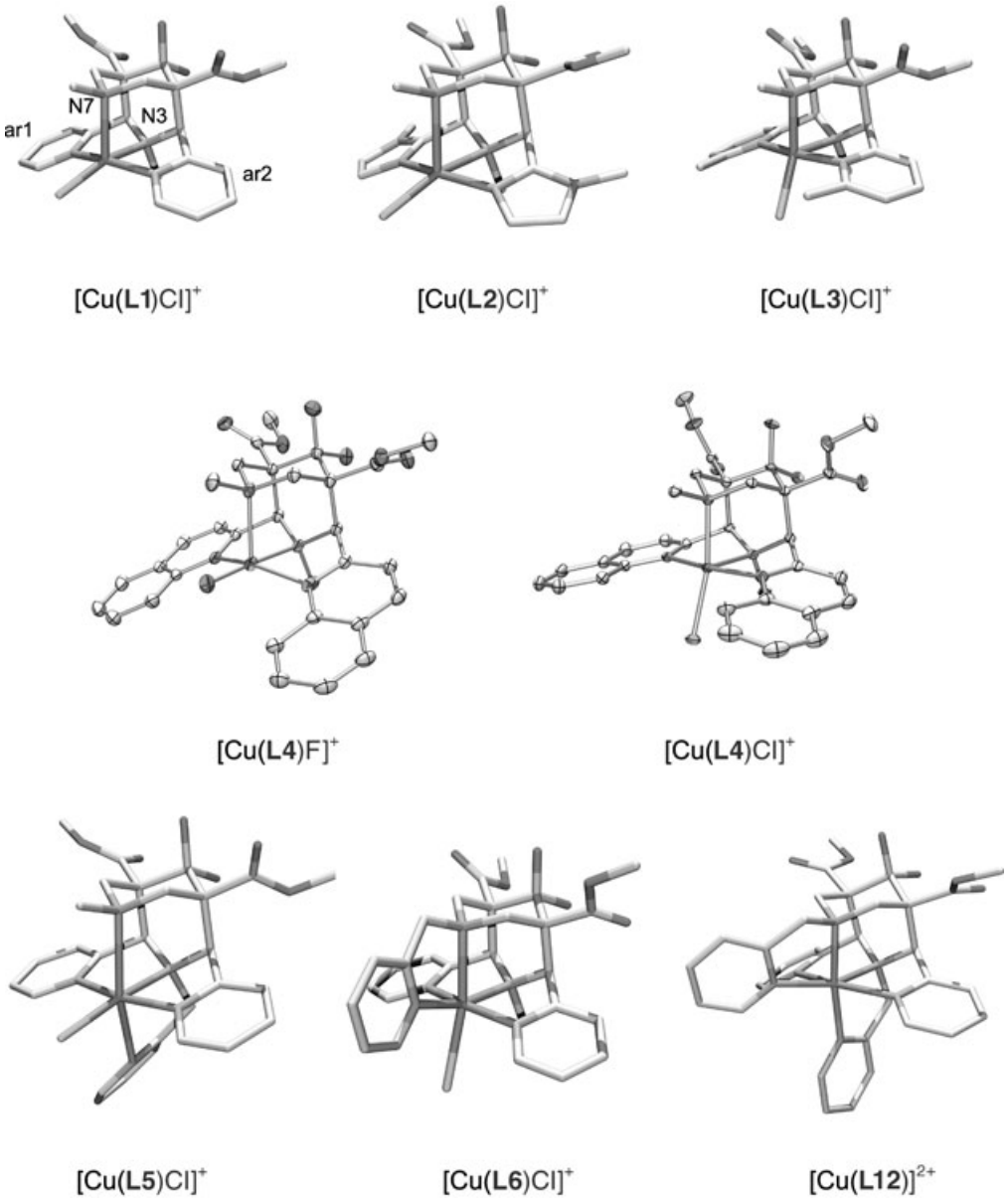

Fig. 2. *Plots of the molecular cations of [Cu^{II}(bispidine)] complexes.* ORTEP[36] plots of the new structures are given; the other structures have been published (see *Table 1* for ref.). The *IUPAC* numbering is given in the plot of [Cu(**L1**)Cl]$^+$ (see *Table 1* for the crystallographic numbering). Ketone or hydrate form at C(9) (MeO–C(9)–OH in case of **L9**).

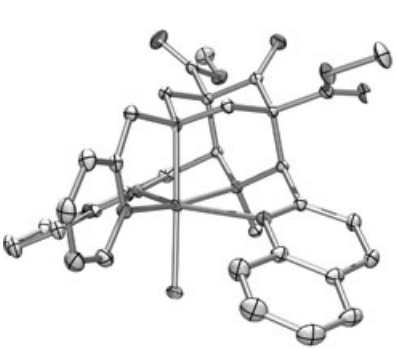

[Cu(**L9**)Cl]$^+$

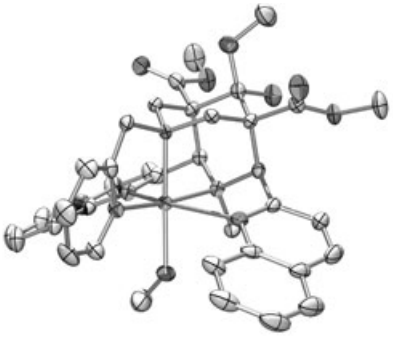

[Cu(**L9**)OMe]$^+$

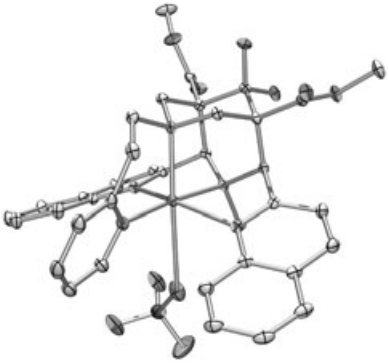

[Cu(**L10**)FBF_3]$^+$

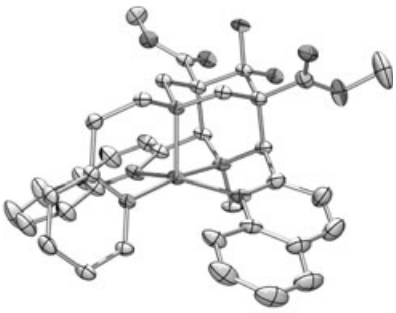

[Cu(**L10**)]$^{2+}$

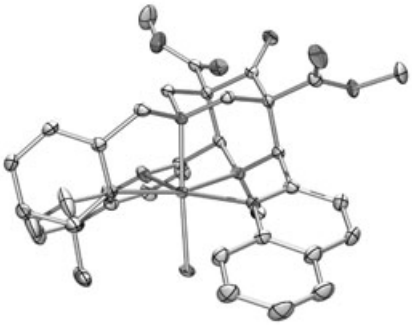

[Cu(**L11**)Cl]$^+$

Fig. 2 (cont.)

unsubstituted pyridine donors but, in addition, there are significant electronic differences in the entire series of aromatic N-donors discussed here (*e.g.*, pK_a: 1*H*-imidazole, 6.99; 2-methylpyridine, 6.00; pyridine, 5.23; quinoline, 4.90). The structural data in *Table 1* indicate qualitatively that, as expected, the quinoline-Cu^{II} bonds are weaker than those with pyridine. Together with steric effects, this leads in general to an elongation along the ar1–Cu–ar2 axis. Only the structure with **L4** and the small F-donor as a co-ligand has an elongated Cu–N(7) bond. With the bulkier Cl^- as a fifth ligand, **L4** has a square-pyramidal geometry with N(3) as the apical donor, similar to the corresponding structure with **L3** [7]. This indicates that, as expected, there is considerable steric hindrance in the plane of the *trans*-disposed quinoline donors. The two alternatives to accommodate bulky co-ligands are a (partially quenched) *Jahn–Teller* elongation along Cu–N(3), as observed in $[Cu^{II}(\mathbf{L4})Cl]^+$ or an elongation involving the two quinoline donors (structures with **L9**, **L10**, and **L11**). The latter structural type is facilitated by the relatively weak quinoline-Cu^{II} bonds.

Of particular interest are the two structures with **L10**. These correspond to a fourth, unexpected and unprecedented structural type. While all other complexes have, as expected, relatively short bonds to the (in-plane) co-ligands, those with **L10** have two long quinoline-Cu^{II} bonds (although the sum of the two bonds is considerably shorter than for the other structures, see structural data of the complexes with ligands **L9** and **L11** in *Table 1*) but only a very weak interaction to the 'in-plane' FBF_3^- co-ligand or a genuinely five-coordinate structure with one 'missing in-plane donor'. Inspection of the angular distribution of the donors indicates that, for the complexes with **L10**, apart from the N(7)–Cu–N(ar3) angle (six- *vs.* five-membered chelate ring), there is not much of a difference with respect to the other structures discussed here. On the basis of an approximate pseudo-octahedral geometry, this indicates that the warped rim of the 'Mexican hat' potential-energy surface has more than three minima (these generally correspond to the three possible tetragonally elongated structures, the saddle points are the correspondingly compressed forms, and the intermediate structures are linear combinations which also involve the Q_ε (in addition to the Q_ϑ) vibrational mode [3][21][22][28]). This is further support for a flat potential-energy surface with bispidine complexes leading to metastable structures. Factors which might be partially responsible for the stabilization of the observed structures are lattice strain (packing forces), the influence of the extended π-clouds of the significantly bent-down quinoline rings, and steric interactions of the pyridine donor ar3 which, for the structures with **L10**, has a very short bond to the Cu^{II} center. Also, it might not be entirely appropriate to describe bispidine coordination complexes as pseudo-octahedral. This also emerges from the study of the thermodynamic stabilities of various bispidine complexes which do not follow the usual *Irving–Williams*-type behavior (*e.g.*, specific stabilization of the d^{10} Zn^{II} complexes [4][29]). For the complexes with **L10** rather low stability constants are expected (see also redox potentials).

Spectroscopy and Electrochemistry. From the structural data it emerges that there are four well-defined structural forms for $[Cu(L)(X)]^{n+}$ complexes, and published data of similar compounds indicate that the relative stability within the set of isomers depends on the ligand L and the co-ligands X (anion or solvent) [3][21][22]. Due to the flat potential-energy surfaces, with a given ligand, a change of the solvent or anion can lead to drastic structural changes and concomitant differences in the electrochemical

and spectroscopic properties. Due to the limited solubilities of the ligands and complexes and specific requirements for some of the analytical methods (good glasses for well-resolved EPR spectra, all CVs from solutions in the same medium, *i.e.*, MeCN, *etc.*) a number of different solvents, solvent mixtures, and salts were used for the different experiments. The assignment of the spectra to specific structural forms and co-ligands is, therefore, not unambiguous in all cases. However, the large set of published and new experimental structural data, together with recent thorough analyses based on spectroscopy [21][22] and computational studies (ligand field, force field, DFT), as well as the solid-state and solution electronic spectra, frozen-solution EPR-spectroscopic and room-temperature electrochemical data in a variety of solvents and solvent mixtures (see *Table 2*) lead to a reasonably consistent picture. Of particular interest is the series of EPR spectra of the $[Cu^{II}(\mathbf{L4})]$ complexes in various solvent mixtures (see *Table 2* and *Fig. 3*) which indicate that, depending on the lability of the co-ligand and on the relative stabilities of the corresponding isomers, there is an equilibrium between various structural forms.

In case of the tetradentate bispidine ligands, only the $[Cu(L)(Cl)]^+$ forms with **L1** and **L2** were stable in aqueous solution; with **L3** and **L4**, identical solution UV/VIS and NIR spectra to those in the solid (*i.e.*, those of the chloro complexes) were only observed when excess Cl^- was added to the solutions (supression of solvolysis). This is not unexpected since the $[Cu(L)]^{2+}/Cl^-$ complexation constants in water are 10 orders of magnitude larger for **L1** than for **L3** [9]. Also, the Cu–Cl distance in the complex with **L4** is slightly larger than in that with **L3** (2.27 *vs.* 2.22 Å). The similarity of the solid-state and solution UV/VIS and NIR spectra of the chloro complexes of **L4** and **L3** [22] (excess Cl^- in solutions) indicates that the solid-state and corresponding solution structures are identical (Cl^- *trans* to N(3) for **L1** and **L2**, and *trans* to N(7) for **L3** and **L4**). That is, in these examples, lattice strain is not a determining factor in terms of the structural forms. Solutions of the BF_4^- or $CF_3SO_3^-$ salts of the complexes are assumed to have the solvents (MeCN, MeOH, H_2O) as co-ligands. With **L3**, it is known [22] and with **L4** it is expected that the coordination site of the co-ligand strongly depends on the size of the anion or solvent molecule and that the site and number of co-ligands coordinated determines the structural form. In the spectroscopic analysis of **L3** with a number of co-ligands, it was possible to correlate the structures with the spectroscopic pattern (spin Hamiltonian and ligand-field parameters). The MeCN structure has an elongated Cu–N(7) bond (5-coordinate), the Cl^- structure has an elongated Cu–N(3) bond (5-coordinate, Cl^- *trans* to N(7)), and with OH_2, there are two species, a 5-coordinate structure which is similar to that with Cl^- and a 6-coordinate structure with an elongation probably involving the two pyridine donors [22]. For **L1** and **L2**, based on a large amount of published data [1][3][7][9], there is little doubt that all species reported in *Table 2* have square-pyramidal structures with elongated Cu–N(7) bonds (weak coordination *trans* to N(7) cannot be excluded).

The structural behavior of the complex systems with **L4** may be characterized on the basis of the series of EPR spectra shown in *Fig. 3*. From the two observations that the chloro complex and the triflate salt in MeCN give completely different spectra, and that, in water, both give identical spectra indicates that *Fig. 3*,*a*, is a spectrum of the complex with coordinated MeCN, that *Fig. 3*,*b*, is a spectrum of a complex with coordinated Cl^-, and that *Fig. 3*,*c*, is a spectrum of an aqua complex. The chloro

Table 2. *Redox and Spectroscopic Properties of* $[Cu(\mathbf{L}m)X_q]^{n+}$

$[Cu^{II}(\mathbf{L})]$	X/solvent	E°[mV] *vs.* $Ag/AgNO_3$	Electronic transition [cm^{-1}] (ε [l $mol^{-1}cm^{-3}$])			EPR[a])		
			ν_1	ν_2	ν_3	$g_\parallel$	$g_\perp$	$A_\parallel$ [$10^{-4}cm^{-1}$]
L1[b])	Cl^-		15380	14290 (sh)		2.225	2.050	174
	MeCN	−417	15870			2.245	2.072	172
	MeOH		15150					
	H_2O		15310					
L2[b])	Cl^-		15630	14490 (sh)		2.230	2.070	165
	MeCN	−440	15380			2.250	2.070	168
	MeOH		15040					
L3[c])	Cl^- (solid)		15300		8300	2.242	2.040	162
	MeCN	−98	16300	14300 (sh)	10000	2.245	2.062	165
	MeOH		12740	12050 (sh)				
	H_2O		16100	13700 (sh)	7600			
L4	Cl (MeCN, MeOH)		14970 (100)	11500 (77)		2.305[d])	2.068[d])	147[d])
	Cl (solid)		14190	11160	8300	2.262	2.066	165
						2.276	2.118	152
	OTf (MeOH)		15630 (89)	13890 (sh)		2.321[d])	2.066[d])	148[d])
						2.279	2.070	159
	OTf (MeCN)	−74	16800 (sh)	14090 (115)				
	OTf (solid)		16000	13700	8900			
L5[b])	Cl^-		13840	12820 (sh)		2.255	2.060	160
	MeCN	−489	15040			2.250	2.080	165
	MeOH		14180					
L6[b])	Cl^-		15625			2.250	2.060	170
	MeCN	−603	16000			2.230	2.075	175
	MeOH		16000					
L7	Cl (MeCN, MeOH)	−691, MeCN	13795 (70)			2.275	2.060	158
	Cl (solid)		13800		8930			
	(BF_4) MeCN	−450	14930 (66)			2.273	2.060	158
	MeOH		14390 (57)					
	BF_4 (solid)		14400		8300			
L8	Cl (MeOH)		14285 (61)	12050 (49)		2.294	2.062	152
	Cl (MeCN)		14190 (70)	11980 (74)				
	Cl (solid)		13500	11800	8300			
	(BF_4) MeCN	−94	16370 (100)	14730 (100)		2.295	2.062	152
	MeOH		15750 (59)	14600 (64)				
	BF_4 (solid)		15360	12700	9900			
L9	Cl (MeCN, MeOH)		14290 (55)	13330 (sh)[c])		2.266	2.058	163
	Cl (TiO_2)		14290[c])	13300[c])	9350			
	(BF_4) MeCN	−383	15270 (65)			2.267	2.058	163
	MeOH		15040 (sh)	14600 (53)				
	BF_4 (solid)		15270[c])	13570[c])	8930			
L10	Cl (MeOH)		15270 (60)	14700 (64)		2.290	2.064	158
	Cl (solid)		13420	12580 (sh)	8480			
	(BF_4) MeCN	−78	15500 (96)	14930 (95)		2.290	2.064	157
	MeOH		15250 (64)	14580 (65)				
	BF_4 (solid)		15390	13990				
L11	Cl (MeCN, MeOH)		14500 (75)			2.292	2.060	152
	(BF_4) MeCN	−69	15750 (83)	14500 (94)		2.291	2.060	152
	MeOH		15390 (41)	12660 (45)				
	BF_4 (solid)		15750	12660	10200 (sh)[c])			
L12		−573 (MeCN)	16130 (110)			2.207	2.077	170

[a]) DMF/H_2O 2 : 3, where not indicated otherwise. [b]) [7]. [c]) [7][23]. [d]) DMF/MeCN 3 : 2.

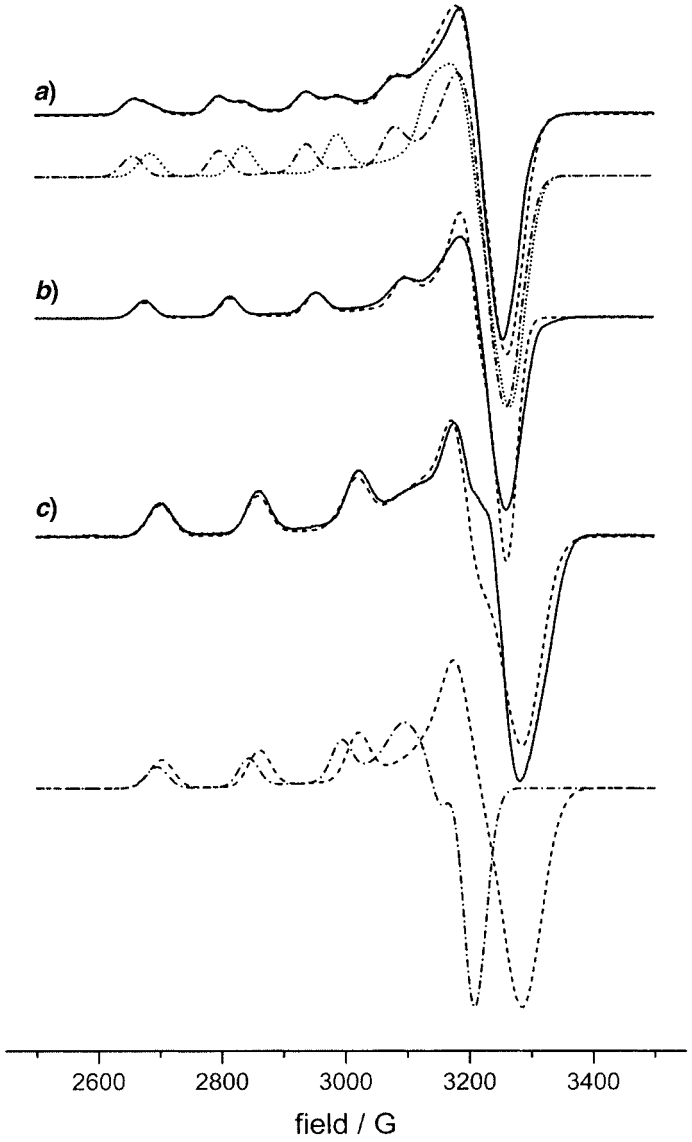

Fig. 3. *EPR Spectra of [Cu(***L4***)(X)$_q$]$^{n+}$* ($q = 1,2$; frozen solution (110 K); X-band; simulations (dotted lines) with XSophe [32][33] (see *Table 2* for parameters)): *a*) *trifluoromethanesulfonate salt in MeCN/DMF 2:3* (simulation of 2 complexes, see text, *Table 2*), *b*) *chloro complex as chloride salt in MeCN/DMF 2:3*, and *c*) *chloro complex as chloride salt or trifluoromethanesulfonate salt* (identical spectra) *in DMF/H_2O 2:3*

complex leads to a clean spectrum of a single species, and the structure probability is identical to that in the crystal (see above, see electronic spectra in *Table 2*). The small value of $A_{||}$ and the large shift of $\Delta g_{||}$ are consistent with a weak ligand field due to the quenched *Jahn–Teller* effect (Cl^- *trans* to N(7), axial N(3)) and relatively weak in-

plane bonds. In MeCN/DMF mixtures (various ratios, *Fig. 3,a*), there are always two species present with various populations. The major species with an intermediate $A_{||}$ ($159 \cdot 10^{-4}\,cm^{-1}$) probably has an elongated Cu–N(7) bond and an in-plane coordinated MeCN donor. There are various possibilities for the second 'isomer' (*e.g.*, an elongation along Cu–N(3)). The spectra in DMF/H_2O (*Fig. 3,c*) may be simulated with a major species with a large value of $A_{||}$ value ($165 \cdot 10^{-4}\,cm^{-1}$) and a minor impurity. The major species probably has an elongated Cu–N(7) bond and a OH_2 coordinated in-plane, the other probably has the quinoline–Cu–quinoline axis elongated and two coordinated OH_2. It appears that, while **L1** and **L2** lead to structurally well-defined complexes, the structures of the Cu^{II} complexes **L3** [22] and **L4** are metastable and, depending on the solvent and added anions, there are subtle structural changes. This is also in agreement with the corresponding electronic spectra. These are not discussed here in detail since the spectral resolution does not allow to thoroughly analyze isomer mixtures. Also, even for apparently isomerically pure samples, the resolution into the expected four transitions is not possible in the powder (reflectance) and solution samples, and the corresponding assignments are not unambiguous. However, the solid-state measurements clearly indicate that there are two different structural forms.

The redox potentials are grouped in two sets. Those of **L1** and **L2** which are 5-coordinate with an elongated Cu–N(7) bond are very negative, *i.e.*, the +2 oxidation state is highly stabilized – **L1** and **L2** are known to form very stable Cu^{II} complexes [4][29]. With **L3**, there is partial quenching of the *Jahn–Teller* stabilization [3][7][22] and a concomitant destabilization of the Cu^{II} complexes. This must also apply for **L4** which, in addition, has a weaker ligand field (lower basicity, nucleophilicity, see above; see also electronic spectra in *Table 2*).

With pentadentate bispidine ligands, there are a number of possible isomeric forms (see discussion of the structural data). Ligands **L5**, and **L6** are isomers and enforce strongly different structures (see *Fig. 2*) with a strong (**L5**) or a weak (**L6**) bond to the co-ligand; correspondingly, complexes with **L6** generally have a much stronger ligand field (see redox potentials, electronic and EPR spectroscopic parameters in *Table 2*). Also, with **L5** and corresponding derivatives, *Jahn–Teller* metastability was first observed, and with the parent ligand **L5** the Cu^{II} complex with MeCN has an elongation involving the two pyridine donors (the chloro complex has the elongation along the axis involving N(7), see *Table 1*) [21]. All other ligands **L7**–**L11** have a topology similar to that of **L6**. However, with the bulkier aromatic N-donors at C(2) and C(4) (ar1, ar2), these all have pseudo-*Jahn–Teller* elongations along the ar1–Cu–ar2 axis (the structures of the complexes with **L7** and **L8** are not known from single-crystal structural analysis but by analogy, preliminary computational studies, and comparison of the spectroscopic properties, these are assumed to be similar). Although the co-ligands are pseudo-in-plane, these are significantly longer than those with the tetradentate ligands **L1** and **L2** and believed to be less-strongly coordinated. The spectroscopic data indicate that in solvent mixtures with H_2O present, the co-ligands (*e.g.*, Cl^-) are substituted (see EPR data in DMF/H_2O, chloride *vs.* triflate salts), while in MeOH or MeCN (see electronic spectroscopy, solution *vs.* solid), Cl^- is not substituted.

The redox potentials are grouped into two sets with strongly negative (−400 to −600 mV for **L5**, **L6**, **L7**, and **L9**) or more-positive potentials (> −100 mV for **L8**, **L10**,

and **L11**). The lower stabilities of the oxidized form (more positive potentials) seems to be a result of the third aromatic N-donor (in-plane with the two quinoline moieties, methyl-substituted pyridine or six-membered chelate ring). The observation that, in general, the solid-state and solution electronic spectra are similar and that all EPR spectra are of single species, the structures in solution are assumed to be all similar, *i.e.*, with elongations along ar1–Cu–ar2 (except for **L5** and **L6**). There is no obvious correlation between the ligand-field properties (electronic and EPR spectra) and the redox potentials. This is not entirely unexpected due to the differences in σ- and π-contributions to the bonding of the different aromatic N-donors.

Financial support by the *German Science Foundation* (*DFG*) is gratefully acknowledged.

Experimental Part

General. Chemicals (*Aldrich*, *Fluka*, *Merck*) were used without further purification; solvents were dried by standard methods; solvents for cyclovoltammetry and spectroscopy were of the highest possible grade and used as purchased. The N,6-dimethylpyridin-2-amine was prepared as described [30][31], the other aldehyde and amine components used for ligand synthesis were commercially available. Electronic spectra: *Varian Cary-1E* spectrophotometer (solns., 1-cm quartz cells) or *Jasco V-570* instrument (diffused reflectance, TiO_2 pellets); λ max in nm, ε in M^{-1} cm^{-1}. IR Spectra: *Perkin-Elmer 16-PC-FTIR* spectrometer; samples dispersed in KBr discs; in cm^{-1}. NMR Spectra: at 200 (^1H) and 50.3 MHz (^{13}C), *Bruker AS-200* instrument; $SiMe_4$ or the solvent as internal reference; δ in ppm, J in Hz. EPR Measurements. *Bruker ELEXSYS-E-500* instrument (usually DMF/H_2O 2:1; for other media, see *Results and Discussion*; at 125 K); the spin-Hamiltonian parameters were obtained by simulation of the spectra with Xsophe [32][33]. Electrochemical measurements: *BAS-100B* workstation with a three-electrode setup consisting of a glassy carbon working electrode, a Pt-wire as the auxiliary electrode, and an $Ag/AgNO_3$ reference electrode (0.1M $Bu_4N(BF_4)$; solns. purged with N_2 before measurement; scan rate 100 mV/s; the reduction potentials are reported with respect to $Ag/AgNO_3$. Mass spectra: *Finnigan 8400* instrument; Nibeol = 4-nitrobenzyl alcohol. Elemental analyses were obtained performed in the analytical laboratories of the chemical institutes of the University of Heidelberg.

Piperidinones **pL***n: General Procedure.* As described for other piperidinone precursors [7][14][26]: To a soln. of dimethyl 3-oxopentanedioate in MeOH is added at 0° and under stirring within *ca.* 5 min the corresponding aldehyde (2 equiv.) and an 41% aq. soln. of methanamine in a slight excess. The red-orange to red-brown mixtures produce, when left stirring at r.t., a yellowish precipitate. This is filtered, washed with MeOH and dried under vacuum: white or slightly yellowish products.

1-Methyl-2,6-bis(6-methylpyridin-2-yl)-4-oxo-piperidine-3,5-dicarboxylic Acid Dimethyl Ester (**pL3**) [23]. To a soln. of dimethyl 3-oxopentanedioate (3 ml, 20.6 mmol) in MeOH (8 ml) is added at 0°, during *ca.* 5 min, 6-methyl-pyridine-2-carboxaldehyde (5 g, 41.3 mmol). Then a 41% aq. $MeNH_2$ soln. (2.16 ml, 24.7 mmol) is added. The mixture turns red-brown, and when it is left stirring opened to air, a pale yellow solid appears after some time. This solid is filtered, washed with MeOH (→ white product), and dried: 5.1 g (60%) of **pL3**. IR: 2986, 2945 (C–H str.); 2814 (*Bohlmann* band); 1726, 1648 (C=O); 1590, 1574 (arom. C–C str.). ^1H-NMR (200 MHz, $CDCl_3$): 3.60, 3.74 (MeO (keto and enol)); 3.90–4.90 (aliph. H); 6.90–7.70 (arom. H); 12.4 (*s*, OH (enol.)). ^{13}C-NMR (50.32 MHz, $CDCl_3$): 38.0, 44.5 (Me–N(1) (keto and enol)); 52.6, 52.5, 52.1, 51.8 (MeO (keto and enol)); 172.2, 171.4, 169.5, 167.2 (C=O (ester of keto and enol)); 202.1 (C(4)=O). Anal. calc. for $C_{22}H_{25}N_3O_5$: C 64.22, H 6.12, N 10.21; found: C 64.25, H 6.17, N 10.23. FAB-MS (Nibeol; pos.): 411 (M^+).

1-Methyl-4-oxo-2,6-di(quinolin-2-yl)piperidine-3,5-dicarboxylic Acid Dimethyl Ester (**pL4**). As described for **pL3**, with dimethyl 3-oxopentanedioate (2.17 ml, 15 mmol), MeOH (8 ml), quinoline-2-carboxaldehyde (5 g, 31 mmol), and 41% aq. $MeNH_2$ soln. (1.52 ml, 18 mmol): 4.8 g (66%) of **pL4**. Light yellow solid. IR: 3054, 2981, 2946 (C–H str.); 2813 (*Bohlmann* band); 1739, 1724, 1709 (C=O); 1617, 1598, 1566 (arom. C–C str.). ^1H-NMR (200 MHz, $CDCl_3$): 3.58, 3.74, 3.80 (MeO (keto and enol)); 4.20–5.20 (aliph. H); 7.30–8.30 (arom. H); 12.6 (*s*, OH (enol)). ^{13}C-NMR (50.32 MHz, $CDCl_3$): 38.0, 44.5 (Me–N(1) (keto and enol)); 52.6, 52.5, 52.1, 51.8 (MeO (keto and enol)); 172.2, 171.4, 169.5, 167.2 (C=O (ester of keto and enol)); 202.1 (C(4)=O). Anal. calc. for $C_{28}H_{25}N_3O_5$: C 69.55, H 5.21, N 8.69; found: C 69.63, H 5.27, N 8.73. FAB-MS (Nibeol; pos.): 485 ($[M+H]^+$).

Bispidinones: General Procedure. To a suspension of the piperidinone in MeOH or EtOH is added at r.t. a 37% aq. formaldehyde soln. Then, the desired amine is added to the mixture which is refluxed for 30–60 min. The mixtures produce, when left at r.t., a white to yellowish precipitate. This is filtered, washed with MeOH, and dried under vacuum: white or slightly yellowish products.

3,7-Dimethyl-9-oxo-2,4-di(quinolin-2-yl)-3,7-diazabicyclo[3.3.1]nonane-1,5-dicarboxylic Acid Dimethyl Ester (**L4**). To a suspension of piperidinone **pL4** (1.5 g, 3.1 mmol) in MeOH (20 ml) is added at r.t. a 37% aq. formaldehyde soln. (0.6 ml, 8.07 mmol). Then a 41% aq. $MeNH_2$ soln. (0.33 ml, 3.94 mmol) is added, and the mixture is refluxed for 1 h. The color gets pale yellow. After refluxing, the mixture is cooled down with the flask opened to air. After one night, a white solid has appeared, which is filtered and washed with MeOH. This solid is a mixture of the desired and nondesired conformation of the bispidinone and is refluxed again for 1 h. Then, the suspension formed is filtered hot, and the solid filtered, collected, and dried: 0.7 g (42%) of **L4**. IR: 3056, 2946 (C–H str.); 2843, 2792 (*Bohlmann* bands); 1734 (C=O); 1617, 1596, 1560, 1502 (arom. C–C str.). ^{1}H-NMR (200 MHz, $CDCl_3$): 2.14 (*s*, Me–N(3)); 2.32 (*s*, Me–N(7)); 2.52 (*d*, ^2J = 12, H_{ax}–C(6), H_{ax}–C(8)); 2.98 (*d*, ^2J = 12, H_{eq}–C(6), H_{eq}–C(8)); 3.93 (*s*, 2 MeO); 4.99 (*s*, H–C(2), H–C(4)); 7.55 (*dd*, ^3J = 7.0, ^4J = 1.1, 1 arom. H); 7.58 (*dd*, ^3J = 7.0, ^4J = 1.1, 1 arom. H); 7.70 (*dd*, ^3J = 6.8, ^4J = 1.5, 1 arom. H); 7.73 (*dd*, ^3J = 6.6, ^4J = 1.5, 1 arom. H); 7.86 (*dd*, ^3J = 8.1, ^4J = 0.8, 2 arom. H); 7.99 (*d*, ^3J = 8.1, 2 arom. H); 8.30 (*d*, ^3J = 8.5, 2 arom. H); 8.37 (*d*, ^3J = 8.5, 2 arom. H). ^{13}C-NMR (50.32 MHz, $CDCl_3$): 43.3, 44.2 (Me–N(3), Me–N(7)); 52.2 (MeO); 60.9 (C(6), C(8)); 62.2 (C(1), C(5)); 74.0 (C(2), C(4)); 168.2 (C=O (ester)); 203.2 (C(9)=O). Anal. calc. for $C_{31}H_{30}N_4O_5$: C 69.13, H 5.61, N 10.40; found: C 68.93, H 5.86, N 10.38. FAB-MS (Nibeol; pos.): 540 ($[M+H]^+$).

3-Methyl-2,4-bis(6-methylpyridin-2-yl)-9-oxo-7-(pyridin-2-ylmethyl)-3,7-diazabicyclo[3.3.1]nonane-1,5-dicarboxylic Acid Dimethyl Ester (**L7**). As described for **L4**, with piperidinone **pL7** (2.0 g, 4.86 mmol), MeOH (25 ml), 37% aq. formaldehyde soln. (0.94 ml, 12.6 mmol), and 2-picolylamine (= pyridine-2-methanamine; 0.63 ml, 6.2 mmol) for 30 min: 1.45 g (55%) of **L7**. IR: 2976, 2941 (C–H str.); 2842, 2812 (*Bohlmann* bands); 1734, 1723 (C=O); 1592, 1573 (arom. C–C str.). ^{1}H-NMR (200 MHz, $CDCl_3$): 1.98 (*s*, Me–N(3)); 2.36 (*s*, 2 Me–C(6)); 2.57 (*d*, ^2J = 11.7, H_{ax}–C(6), H_{ax}–C(8)); 2.98 (*d*, ^2J = 11.7, H_{eq}–C(6), H_{eq}–C(8)); 3.49 (*s*, CH_2–N(7)); 3.76 (*s*, 2 MeO); 4.58 (*s*, H–C(2), H–C(4)); 6.92 (*d*, ^3J = 7.6, 2 arom. H); 7.15–7.30 (*m*, 2 arom. H); 7.36 (*t*, ^3J = 7.6, 2 arom. H); 7.50–7.75 (*m*, 3 arom. H); 8.57 (*d*, ^3J = 4, 1 arom. H). ^{13}C-NMR (50.32 MHz, $CDCl_3$): 43.1 (Me–N(3)); 52.0 (MeO); 58.6 (C(6), C(8)); 62.2 (C(1), C(5)); 63.3 (Me–N(7)); 73.5 (C(2), C(4)); 168.5 (C=O (ester)); 203.4 (C(9)=O). Anal. calc. for $C_{30}H_{33}N_5O_5$: C 66.28, H 6.12, N 12.88; found: C 66.00, H 6.19, N 12.70. FAB-MS (Nibeol; pos.): 566 ($[M+Na]^+$), 543 (M^+), 485 ($[M-CO_2Me]^+$).

3-Methyl-2,4-bis(6-methylpyridin-2-yl)-7-[(6-methylpyridin-2-yl)methyl]-9-oxo-3,7-diazabicyclo[3.3.1]nonane-1,5-dicarboxylic Acid Dimethyl Ester (**L8**). As described for **L4**, with piperidinone **pL8** (1.1 g, 2.67 mmol), MeOH (15 ml), 37% aq. formaldehyde soln. (0.52 ml, 6.94 mmol), and 6-methylpyridin-2-methanamine (0.35 ml, 3.39 mmol) for 30 min: 0.45 g (30%) of **pL8**. IR: 3057, 2988, 2947 (C–H str.); 2835, 2807 (*Bohlmann* bands); 1730 (C=O); 1592, 1574 (arom. C– str.). ^{1}H-NMR (200 MHz, $CDCl_3$): 2.13 (*s*, Me–N(3)); 2.52 (*s*, 2 Me–C(6) (Py)); 2.67 (*s*, 1 Me–C(6)); 2.80 (*d*, ^2J = 12, H_{ax}–C(6), H_{ax}–C(8)); 3.13 (*d*, ^2J = 12, H_{eq}–C(6), H_{eq}–C(8)); 3.60 (*s*, CH_2–N(7)); 3.91 (*s*, 2 MeO); 4.73 (*s*, H–C(2), H–C(4)); 7.07 (*d*, ^3J = 7.4, 2 arom. H); 7.20 (*d*, ^3J = 7.2, 2 arom. H); 7.49 (*t*, ^3J = 7.6, 2 arom. H); 7.65 (*t*, ^3J = 7.7, 1 arom. H); 7.86 (*d*, ^3J = 7.2, 2 arom. H). ^{13}C-NMR (50.32 MHz, $CDCl_3$): 43.2 (Me–N(3)); 52.0 (MeO); 58.6 (C(6), C(8)); 62.2 (C(1), C(5)); 73.5 (C(2), C(4)); 168.5 (C=O (ester)); 203.5 (C(9)–O). Anal. calc. for $C_{31}H_{35}N_5O_5$: C 66.77, H 6.33, N 12.56; found: C 66.59, H 6.34, N 12.37. FAB-MS (Nibeol; pos.): 559 ($[M+H]^+$).

3-Methyl-9-oxo-7-(pyridin-2-ylmethyl)-2,4-di(quinolin-2-yl)-3,7-diazabicyclo[3.3.1]nonane-1,5-dicarboxylic Acid Dimethyl Ester (**L9**). As described for **L4**, with piperidinone **pL9** (1.5 g, 3.10 mmol), MeOH (20 ml), 37% aq. formaldehyde soln. (0.6 ml, 8.07 mmol), and 2-picolylamine (0.40 ml, 3.94 mmol) for 30 min: 0.97 g (51%) of **L9**. IR: 3061, 2984, 2948 (C–H str.); 2840, 2797 (*Bohlmann* bands); 1754, 1734 (C=O); 1617, 1597, 1570, 1501 (arom. C–C str.). ^{1}H-NMR (200 MHz, $CDCl_3$): 2.01 (*s*, Me–N(3)); 2.65 (*d*, ^2J = 12, H_{ax}–C(6), H_{ax}–C(8)); 3.12 (*d*, ^2J = 12, H_{eq}–C(6), H_{eq}–C(8)); 3.59 (*s*, CH_2–N(7)); 3.81 (*s*, 2 MeO); 4.87 (*s*, H–C(2), H–C(4)); 7.20–7.30 (*m*, 2 arom. H); 7.45 (*dt*, ^3J = 7.9, ^4J = 1.1, 2 arom. H); 7.60 (*dt*, ^3J = 6.8, ^4J = 1.5, 2 arom. H); 7.72 (*d*, ^3J = 8.3, 2 arom. H); 7.87 (*d*, ^3J = 8.4, 2 arom. H); 7.96 (*d*, ^3J = 8.6, 2 arom. H); 8.18 (*d*, ^3J = 8.6, 2 arom. H); 8.68 (*d*, ^3J = 4.3, 1 arom. H). ^{13}C-NMR (50.32 MHz, $CDCl_3$): 43.2 (Me–N(3)); 52.2 (MeO); 58.6 (C(6), C(8)); 62.5 (C(1), C(5)); 63.3 (CH_2–N(7)); 74.1 (C(2), C(4)); 168.2 (C=O (ester)). Anal. calc. for $C_{36}H_{33}N_5O_5$: C 70.23, H 5.40, N 11.38; found: C 69.89, H 5.42, N 11.37. FAB-MS (Nibeol; pos.): 617 ($[M+H]^+$).

3-Methyl-9-oxo-7-[2-(pyridin-2-yl)ethyl]-2,4-di(quinolin-2-yl)-3,7-diazabicyclo[3.3.1]nonane-1,5-dicarboxylic Acid Dimethyl Ester (**L10**). As described for **L4**, with piperidinone **pL10** (1.1 g, 2.27 mmol), MeOH (20 ml), 37% aq. formaldehyde soln. (0.44 ml, 5.9 mmol), and 2-(pyridin-2-yl)ethanamine (0.36 ml, 2.89 mmol) for 90 min. After cooling down to r.t., the mixture is evaporated. The obtained sticky yellow gum is dissolved in

Et_2O (15 ml) and refluxed again for 30 min. After one night with the flask opened to air, the pale yellow solid is filtered off and dried: 0.62 g (43%) of **L10**. IR: 3056, 2948 (C−H str.); 2853, 2813 (*Bohlmann* bands); 1730 (C=O); 1617, 1596, 1568, 1501 (arom. C−C str.). ^{1}H-NMR (200 MHz, $CDCl_3$): 2.05 (*s*, Me−N(3)); 2.59 (*d*, ^2J = 12.5, H_{ax}−C(6), H_{ax}−C(8)); 2.70–3.00 (*m*, CH_2CH_2−N(7)); 3.11 (*d*, ^2J = 12.5, H_{eq}−C(6), H_{eq}−C(8)); 3.86 (*s*, 2 MeO); 4.90 (*s*, H−C(2), H−C(4)); 7.05–7.15 (*m*, 2 arom. H); 7.40–7.70 (*m*, 5 arom. H); 7.78 (*dd*, ^3J = 8.2, ^4J = 1, 2 arom. H); 7.91 (*d*, ^3J = 8.5, 2 arom. H); 8.20 (*d*, ^3J = 8.6, 2 arom. H); 8.28 (*d*, ^3J = 8.6, 2 arom. H); 8.52 (*m*, 1 arom. H). ^{13}C-NMR (50.32 MHz, $CDCl_3$): 43.3 (Me−N(3)); 52.3 (MeO); 57.1 (CH_2CH_2−N(7)); 58.6 (C(6), C(8)); 62.2 (C(1), C(5)); 73.9 (C(2), C(4)); 168.2 (C=O (ester)). Anal. calc. for $C_{37}H_{35}N_5O_5$: C 70.57, H 5.60, N 11.12; found: C 69.60, H 5.73, N 11.24. FAB-MS (Nibeol; pos.): 631 ($[M+H]^+$).

3-Methyl-7-[(6-methylpyridin-2-yl)methyl]-9-oxo-2,4-di(quinolin-2-yl)-3,7-diazabicyclo[3.3.1]nonane-1,5-dicarboxylic Acid Dimethyl Ester (**L11**). As described for **L4**, with piperidinone **pL11** (1.15 g, 2.38 mmol), MeOH (15 ml), 37% aq. formaldehyde soln. (0.46 ml, 6.18 mmol), and 6-methylpyridin-2-methanamine (0.35 ml, 3.39 mmol) 1 h. After cooling with the flask opened to air, and after two days, the white solid (mixture of isomers) is collected and refluxed again for 30 min in MeOH. The suspension formed is filtered hot and the collected solid dried: 0.45 g (25%) of **L11**. IR: 3058, 2983, 2949 (C−H str.); 2842, 2804 (*Bohlmann* bands); 1737, 1724 (C=O); 1617, 1597, 1577, 1501 (C−C str.). ^{1}H-NMR (200 MHz, $CDCl_3$): 2.01 (*s*, Me−N(3)); 2.59 (*s*, Me−C(6) (Py)); 2.65 (*d*, ^2J = 12.6, H_{ax}−C(6), H_{ax}−C(8)); 3.11 (*d*, ^2J = 12.6, H_{eq}−C(6), H_{eq}−C(8)); 3.52 (*s*, CH_2−N(7)); 3.82 (*s*, 2 MeO); 4.86 (*s*, H−C(2), H−C(4)); 7.00–7.20 (*m*, 2 arom. H); 7.53 (*dd*, ^3J = 7.0, ^4J = 1.1, 1 arom. H); 7.56 (*dd*, ^3J = 7.0, ^4J = 1.1, 1 arom. H); 7.67 (*dd*, ^3J = 7.0, ^4J = 1.5, 1 arom. H); 7.70 (*dd*, ^3J = 7.0, ^4J = 1.5, 1 arom. H); 7.81 (*dd*, ^3J = 8.1, ^4J = 1.1, 2 arom. H); 7.95 (*d*, ^3J = 7.4, 2 arom. H); 8.02 (*d*, ^3J = 8.5, 2 arom. H); 8.30 (*d*, ^3J = 9.2, 2 arom. H). ^{13}C-NMR (50.32 MHz, $CDCl_3$): 43.2 (Me−N(3)); 52.2 (MeO); 58.9 (C(6), C(8)); 62.5 (C(1), C(5)); 74.1 (C(2), C(4)); 168.1 (C=O (ester)). Anal. calc. for $C_{37}H_{35}N_5O_5$: C 70.57, H 5.60, N 11.12; found: C 70.36, H 5.72, N 11.06. FAB-MS (Nibeol; pos.): 653 ($[M+Na]^+$), 631 ($[M+H]^+$).

Copper(II) Complexes: General Procedure. A suspension of the ligand (*ca.* 150 to 200 mg) in MeOH is mixed with the soln. of a copper salt ($CuCl_2 \cdot 2\,H_2O$ or $Cu(BF_4)_2 \cdot 6\,H_2O$) in the same solvent. Most of the complex formations lead to clear solns., in some cases the product precipitates. The colors observed are various shades between deep blue and green. To precipitate the complexes from the solns., Et_2O is added. The collected solids are filtered and dried.

*Chloro[dimethyl 3,7-Dimethyl-9-oxo-2,4-bis(quinolin-2-yl-κN)-3,7-diazabicyclo[3.3.1]nonane-1,5-dicarboxylate-κN^3,κN^7]copper(2+) Chloride Trihydrate ([Cu(***L4***)Cl]Cl · 3 H_2O):* UV/VIS (MeOH): 668 (100), 870 (77). UV/VIS (MeCN): 668 (100), 870 (77). UV/VIS (TiO_2): 705, 896, 1200. IR: 3054, 3007, 2950 (C−H str.); 1728 (C=O); 1617, 1595, 1569, 1507 (arom. C−C str.). Anal. calc. for $C_{31}H_{30}Cl_2CuN_4O_5 \cdot 3\,H_2O$: C 52.51, H 4.83, N 7.90; found: C 51.99, H 5.13, N 7.58. FAB-MS (Nibeol; pos.): 620 ($[Cu\mathbf{L4}+H_2O]^+$).

*Dimethyl 3,7-Dimethyl-9-oxo-2,4-bis(quinolin-2-yl-κN)-3,7-diazabicyclo[3.3.1]nonane-1,5-dicarboxylate-κN^3,κN^7](trifluoromethanesulfonato-κO)copper(2+) Trifluoromethane Sulfonate Hydrate Methanol ([Cu(***L4***)OTf]OTF · H_2O · MeOH).* UV/VIS (MeOH): 640 (89), 720 (sh). UV/VIS (MeCN): 595 (sh), 710 (115). UV/VIS (TiO_2): 625, 730, 1125. CV (MeCN): $E_{1/2} = -74$ mV ($\Delta E = 77$ mV). Anal. calc. for $C_{34}H_{36}CuF_6N_4O_{13}S_2$: C 42.97, H 3.82, N 5.90; found: C 42.71, H 4.03, N 5.91.

*Chloro{dimethyl 3-Methyl-2,4-bis(6-methylpyridin-2-yl-κN)-9-oxo-7-[(pyridin-2-yl-κN)methyl]-3,7-diazabicyclo[3.3.1]nonane-1,5-dicarboxylate-κN^3,κN^7}copper(2+) Chloride Trihydrate ([Cu(***L7***)Cl]Cl · 3 H_2O).* UV/VIS (MeOH): 725 (70). UV/VIS (MeCN): 725 (70). UV/VIS (TiO_2): 725, 1120. IR: 3062, 2950, 2919 (C−H str.); 1734 (C=O); 1599, 1572 (arom. C−C str.). CV (MeCN): $E_{1/2} = -691$ mV ($\Delta E = 184$ mV). EPR (DMF/H_2O 2:1, 125 K): $g_{\|} = 2.275$, $A_{\|} = 158$ G, $g_{\perp} = 2.060$, $A_{\perp} = 9$ G. Anal. calc. for $C_{30}H_{33}Cl_2CuN_5O_5 \cdot 3\,H_2O$: C 49.22, H 5.37, N 9.57; found: C 48.92, H 5.45, N 9.47. FAB-MS (Nibeol; pos.): 643 ($[Cu\mathbf{L7}Cl]^+$), 661 ($[Cu\mathbf{L7}Cl+H_2O]^+$).

*Dimethyl 3-Methyl-2,4-bis(6-methylpyridin-2-yl-κN)-9-oxo-7-[(pyridin-2-yl-κN)methyl]-3,7-diazabicyclo[3.3.1]nonane-1,5-dicarboxylate-κN^3,κN^7}copper(2+) Bis[tetrafluoroborate(1−)] Dihydrate ([Cu(***L7***)][BF_4]$_2$ · 2 H_2O).* UV/VIS (MeOH): 695 (57). UV/VIS (MeCN): 670 (66). UV/VIS (TiO_2): 695, 1200. IR: 3064, 2954, 2916 (C−H str.); 1744, 1715 (C=O); 1599, 1572 (arom. C−C str.). CV (MeCN): $E_{1/2} = -450$ mV ($\Delta E = 87$ mV). EPR (DMF/H_2O 2:1, 125 K): $g_{\|} = 2.273$, $A_{\|} = 158$ G, $g_{\perp} = 2.060$, $A_{\perp} = 9$ G. Anal. calc. for $C_{30}H_{33}B_2CuF_8N_5O_5 \cdot 2\,H_2O$: C 44.11, H 4.57, N 8.57; found: C 44.34, H 4.78, N 8.45. FAB-MS (Nibeol; pos.): 643 ($[Cu\mathbf{L7}Cl+2\,H_2O]^+$), 661 ($[Cu\mathbf{L7}Cl+3\,H_2O]^+$).

*Chloro[dimethyl 3-Methyl-2,4-bis(6-methylpyridin-2-yl-κN)-7-[(6-methylpyridin-2-yl-κN)methyl]-9-oxo-3,7-diazabicyclo[3.3.1]nonane-1,5-dicarboxylate-κN^3,κN^7]copper(2+) Chloride Hydrate ([Cu(***L8***)Cl]Cl · H_2O).* UV/VIS (MeOH): 700 (61), 830 (49). UV/VIS (MeCN): 705 (70), 835 (74). UV/VIS (TiO_2): 742, 850, 1210. IR: 3048, 3000, 2952 (C−H str.); 1730 (C=O); 1600, 1573 (arom. C−C str.). EPR (DMF/H_2O 2:1,

125 K): $g\,||=2.294$, $A\,||=152$ G, $g_\perp=2.062$, $A_\perp=9$ G. Anal. calc. for $C_{31}H_{35}Cl_2CuN_5O_5\cdot 1\ H_2O$: C 52.43, H 5.25, N 9.86; found: C 52.46, H 5.29, N 9.79. FAB-MS (Nibeol; pos.): 621 ([Cu**L8**]$^+$), 657 ([Cu**L8**Cl]$^+$).

*{Dimethyl 3-Methyl-2,4-bis(6-methylpyridin-2-yl-κN)-7-[(6-methylpyridin-2-yl-κN)methyl]-9-oxo-3,7-diazabicyclo[3.3.1]nonane-1,5-dicarboxylate-κN^3,κN^7}copper(2+) Bis[tetrafluoroborate(1−)] Dihydrate ([Cu(**L8**)][BF$_4$]$_2\cdot 2\ H_2O$)*. UV/VIS (MeOH): 635 (59), 685 (64). UV/VIS (MeCN): 611 (100), 679 (100). UV/VIS (TiO_2): 651, 790, 1010. IR: 2951 (C−H str.); 1728 (C=O); 1605, 1574 (arom. C−C str.). CV (MeCN): $E_{1/2}=-94$ mV ($\Delta E=75$ mV). EPR (DMF/H_2O 2:1, 125 K): $g_{||}=2.295$, $A_{||}=152$ G, $g_\perp=2.062$, $A_\perp=9$ G. Anal. calc. for $C_{31}H_{35}B_2CuF_8N_5O_5\cdot 2\ H_2O$: C 44.81, H 4.73, N 8.43; found: C 44.70, H 4.96, N 8.29. FAB-MS (Nibeol; pos.): 621 ([Cu**L8**]$^+$), 639 ([Cu**L8** + H_2O]$^+$), 657 ([Cu**L8** + 2 H_2O]$^+$).

*Chloro{dimethyl 3-Methyl-9-oxo-7-[(pyridin-2-yl-κN)methyl]-2,4-bis(quinolin-2-yl-κN)-3,7-diazabicyclo[3.3.1]nonane-1,5-dicarboxylate-κN^3,κN^7}copper(2+) Chloride Trihydrate ([Cu(**L9**)Cl]Cl$\cdot 3\ H_2O$)*. UV/VIS (MeOH): 700 (55), 750 (sh). UV/VIS (MeCN): 700 (55), 750 (sh). UV/VIS (TiO_2): 700, 750, 1070. IR: 3057, 2997, 2943 (C−H str.); 1723 (C=O); 1608, 1593, 1569, 1504 (arom. C−C str.). EPR (DMF/H_2O 2:1, 125 K): $g_{||}=2.266$, $A_{||}=163$ G, $g_\perp=2.058$, $A_\perp=9$ G. Anal. calc. for $C_{36}H_{33}Cl_2CuN_5O_5\cdot 3\ H_2O$: C 53.77, H 4.89, N 8.71; found: C 53.83, H 4.85, N 8.66. FAB-MS (Nibeol; pos.): 697 ([Cu**L9** + H_2O]$^+$), 733 ([Cu**L9**Cl + H_2O]$^+$).

*{Dimethyl 3-Methyl-9-oxo-7-[(pyridin-2-yl-κN)methyl]-2,4-bis(quinolin-2-yl-κN)-3,7-diazabicyclo[3.3.1]nonane-1,5-dicarboxylate-κN^3,κN^7}copper(2+) Bis[tetrafluoroborate(1−)] Dihydrate ([Cu(**L9**)][BF$_4$]$_2\cdot$ 2 H_2O)*. UV/VIS (MeOH): 665 (sh), 685 (53). UV/VIS (MeCN): 655 (65). UV/VIS (TiO_2): 655, 737, 1120. IR: 3064, 2953 (C−H str.); 1730 (C=O); 1610, 1595, 1571, 1507 (arom. C−C str.). CV (MeCN): $E_{1/2}=-383$ mV ($\Delta E=78$ mV). EPR (DMF/H_2O 2:1, 125 K): $g_{||}=2.267$, $A_{||}=163$ G, $g_\perp=2.058$, $A_\perp=9$ G. Anal. calc. for $C_{36}H_{33}B_2CuF_8N_5O_5\cdot 2\ H_2O$: C 47.68, H 4.33, N 7.72; found: C 48.07, H 4.34, N 7.73. FAB-MS (Nibeol; pos.): 780 ([Cu**L9**(BF$_4$)]$^+$).

*Chloro{dimethyl 3-Methyl-9-oxo-7-[2-(pyridin-2-yl-κN)ethyl]-2,4-bis(quinolin-2-yl-κN)-3,7-diazabicyclo[3.3.1]nonane-1,5-dicarboxylate-κN^3,κN^7}copper(2+) Chloride Trihydrate ([Cu(**L10**)Cl]Cl$\cdot 3\ H_2O$)*. UV/VIS (MeOH): 655 (60), 680 (64). UV/VIS (TiO_2): 745, 795 (sh), 1180. IR: 3040, 3002, 2949, 2914 (C−H str.); 1721 (C=O); 1607, 1595, 1568, 1507 (arom. C−C str.). EPR (DMF/H_2O 2:1, 125 K): $g_{||}=2.290$, $A_{||}=158$ G, $g_\perp=2.064$, $A_\perp=9$ G. Anal. calc. for $C_{37}H_{35}Cl_2CuN_5O_5\cdot 3\ H_2O$: C 54.31, H 5.05, N 8.56; found: C 53.91, H 5.13, N 8.97. FAB-MS (Nibeol; pos.): 693 ([Cu**L10**]$^+$).

*{Dimethyl 3-Methyl-9-oxo-7-[2-(pyridin-2-yl-κN)ethyl]-2,4-bis(quinolin-2-yl-κN)-3,7-diazabicyclo[3.3.1]nonane-1,5-dicarboxylate-κN^3,κN^7}copper(2+) Bis[tetrafluoroborate(1−)] Tetrahydrate ([Cu(**L10**)][BF$_4$]$_2\cdot$ 4 H_2O)*. UV/VIS (MeOH): 656 (64), 685 (65). UV/VIS (MeCN): 645 (96), 670 (95). UV/VIS (TiO_2): 650, 715, 1125. IR: 3061, 2955 (C−H str.); 1739, 1716 (C=O); 1610, 1593, 1569, 1508 (arom. C−C str.). CV (MeCN): $E_{1/2}=-78$ mV ($\Delta E=72$ mV). EPR (DMF/H_2O 2:1, 125 K): $g_{||}=2.290$, $A_{||}=157$ G, $g_\perp=2.064$, $A_\perp=9$ G. Anal. calc. for $C_{37}H_{35}B_2CuF_8N_5O_5\cdot 4\ H_2O$: C 47.33, H 4.62, N 7.46; found: C 47.38, H 4.64, N 7.49. FAB-MS (Nibeol; pos.): 693 ([Cu**L10**]$^+$).

*Chloro{dimethyl 3-Methyl-7-[(6-methylpyridin-2-yl-κN)methyl]-9-oxo-2,4-bis(quinolin-2-yl-κN)-3,7-diazabicyclo[3.3.1]nonane-1,5-dicarboxylate-κN^3,κN^7}copper(2+) Chloride Trihydrate ([Cu(**L11**)Cl]Cl$\cdot 3\ H_2O$)*. UV/VIS (MeOH): 690 (75), 820 (60). UV/VIS (MeCN): 690 (75). IR: 3038, 3006, 2946 (C−H str.); 1727 (C=O); 1608, 1595, 1571, 1505 (arom. C−C str.). EPR (DMF/H_2O 2:1, 125 K): $g_{||}=2.292$, $A_{||}=152$ G, $g_\perp=2.060$, $A_\perp=9$ G. Anal. calc. for $C_{37}H_{35}Cl_2CuN_5O_5\cdot 3\ H_2O$: C 53.77, H 4.89, N 8.71; found: C 53.89, H 5.00, N 8.43. FAB-MS (Nibeol; pos.): 693 ([Cu**L11**]$^+$).

*{Dimethyl 3-Methyl-7-[(6-Methylpyridin-2-yl-κN)methyl]-9-oxo-2,4-bis(quinolin-2-yl-κN)-3,7-diazabicyclo[3.3.1]nonane-1,5-dicarboxylate-κN^{3}κN^7}copper(2+) Bis[(tetrafluoroborate(1−)] Dihydrate Methanol ([Cu(**L11**)][BF$_4$]$_2\cdot 2\ H_2O\cdot 1$ MeOH)*. UV/VIS (MeOH): 650 (41), 790 (45). UV/VIS (MeCN): 635 (83), 690 (94). UV/VIS (TiO_2): 635, 750 (sh), 790, 980 (sh). IR: 3053, 3005, 2955 (C−H str.); 1736, 1731 (C=O); 1595, 1572, 1504 (arom. C−C str.). CV (MeCN): $E_{1/2}=-69$ mV ($\Delta E=80$ mV); EPR (DMF/H_2O 2:1, 125 K): $g_{||}=2.291$, $A_{||}=152$ G, $g_\perp=2.060$, $A_\perp=9$ G. Anal. calc. for $C_{37}H_{35}B_2CuF_8N_5O_5\cdot 2\ H_2O\cdot 1$ MeOH: C 48.82, H 4.64, N 7.49; found: C 48.85, H 4.75, N 7.56. FAB-MS (Nibeol; pos.): 693 ([Cu**L11**]$^+$), 711 ([Cu**L11** + H_2O]$^+$), 725 ([Cu**L11** + MeOH]$^+$).

Crystal-Structure Determination. Single crystals of **L8**, **L11**, [Cu(**L4**)(Cl)]$^+$, [Cu(**L4**)(F)]$^+$, [Cu(**L9**)(Cl)]$^+$, [Cu(**L9**)(OCH_3)]$^+$, [Cu(**L11**)(Cl)]$^+$, [Cu(**L10**)(FBF_3)]$^+$, and [Cu(**L10**)]$^{2+}$, appropriate for X-ray structural analysis, were obtained by slow Et_2O diffusion into solns. of the ligands and complexes in MeOH. Crystal data and details of the structure determinations are listed in *Table 3*. Intensity data were collected at low temperature on a *Bruker AXS-SMART-1000* area detector (MoK_α radiation, λ 0.71073 Å, ω-scan). The structures were solved by direct methods and refined by full-matrix least-squares, based on F^2 with all reflections by using the SHELXTL programs [34]. In [Cu(**L4**)F]$^+$, H-atoms were inserted in calculated positions. In the other

Table 3. *Crystal Data*

	L8	**L11**	[Cu(**L4**)Cl]$^+$	[Cu(**L4**)F]$^+$	[Cu(**L9**)Cl]$^+$	[Cu(**L9**)OMe]$^+$	[Cu(**L10**)FBF$_3$]$^+$	[Cu(**L10**)]$^{2+}$	[Cu(**L11**)Cl]$^+$
Empirical formula	$C_{31}H_{35}N_5O_5$	$C_{37}H_{35}N_5O_5$	$C_{31}H_{32}Cl_2CuN_4O_6$	$C_{31}H_{32}BCuF_5N_4O_6$	$C_{38}H_{41}C_{12}CuN_5O_7$	$C_{42}H_{45}B_2CuF_8N_5O_8$	$C_{37}H_{37}B_2CuF_8N_5O_6$	$C_{38}H_{38.5}B_2CuF_8N_{5.5}O_6$	$C_{39}H_{43}Cl_2CuN_5O_7$
M_r	557.64	629.70	691.05	725.96	814.20	984.99	884.88	905.40	828.22
Temperature [°]	103(2)	103(2)	103(2)	103(2)	103(2)	103(2)	103(2)	103(2)	103(2)
Crystal size [mm]	0.38 × 0.22 × 0.10	0.46 × 0.40 × 0.12	0.30 × 0.27 × 0.06	0.33 × 0.23 × 0.15	0.45 × 0.28 × 0.15	0.25 × 0.15 × 0.07	0.25 × 0.24 × 0.06	0.30 × 0.3 × 0.15	0.23 × 0.22 × 0.15
Crystal system	triclinic	monoclinic	triclinic	triclinic	monoclinic	triclinic	monoclinic	triclinic	monoclinic
Space group	*P*-1	$P2_1/c$	*P*-1	*P*-1	$P2_1/c$	*P*-1	$P2_1/c$	*P*-1	$P2_1/c$
Unit-cell dim.: *a* [Å]	9.5806(5)	10.2303(5)	8.4531(3)	11.6040(6)	14.7853(8)	11.810(11)	15.933(8)	12.0013(6)	4.4654(9)
b [Å]	11.3229(6)	29.969(2)	19.1872(8)	12.2298(7)	14.4980(8)	12.386(17)	14.9349(8)	12.9661(7)	15.3580(10)
c [Å]	13.6137(7)	11.2612(6)	21.5141(9)	12.8881(7)	17.3242(9)	15.800(12)	15.2569(8)	14.1462(7)	17.0184(11)
α [°]	89.207(1)	90	98.541(1)	65.483(1)	90	99.35(10)	90	72.363(1)	90
β [°]	75.510(1)	113.248(1)	92.217(1)	88.488(1)	98.443(1)	106.81(5)	94.026(1)	74.443(1)	98.873(1)
γ [°]	85.315(1)	90	97.341(1)	67.417(1)	90	99.13(8)	90	76.467(1)	90
Volume [Å^3]	1424.65(13)	3172.3(3)	3416.5(2)	1517.14(14)	3673.3(3)	2131(4)	3621.7(3)	1992.8(2)	3735.6(4)
Z	2	4	4	2	4	2	4	2	4
Density (calc.) [g cm^{-3}]	1.300	1.318	1.343	1.589	1.472	1.535	1.623	1.509	1.473
Abs. coeff.	0.090	0.089	0.841	0.803	0.798	0.608	0.701	0.639	0.786
F(000)	592	1328	1428	746	1692	1014	1812	928	1724
θ_{max}	32.04	32.02	32.00	32.04	32.03	26.41	32.03	32.03	28.29
Reflections:									
collected	24762	42648	58924	25922	57397	36296	42246	39281	26800
indep. (R_{int})	9607 (0.036)	10830 (0.039)	23001 (0.039)	102231 (0.027)	12663 (0.048)	8679 (0.046)	12366 (0.045)	13459 (0.032)	9262 (0.062)
Parameters	510	561	1039	568	642	764	680	743	617
G.o.f. on F^2	1.019	1.058	1.058	1.053	1.075	1.053	1.020	1.038	1.069
R_1 ($I > 2\sigma(I)$)	0.0482	0.0578	0.0459	0.0589	0.0402	0.0668	0.0416	0.0519	0.0584
wR_2 (all data)	0.1380	0.1648	0.1334	0.1705	0.1148	0.1858	0.1152	0.1512	0.1515
Larg.diff.peak; hole	0.52; −0.24	1.28; −0.50	1.166; −1.854	3.91; −1.28	0.82; −0.50	1.46; −0.71	0.63; −0.49	1.09; −0.68	1.38; −1.48

structures, they were located and refined (except some of the Me groups). In $[Cu(\mathbf{L4})Cl]^+$, disordered solvent molecules could not be refined. A correction of the data was applied with the routine SQUEEZE [35]. CCDC 255791–255799 contain the supplementary crystallographic data for this paper. These data can be obtained free of charge *via* www.ccdc.cam.ac.uk/conts/retrieving.html (or from CCDC, 12 Union Road, Cambridge CB2 1EZ, UK (fax: +44-1223/336-033: e-mail: deposit@ccdc.cam.ac.uk).

REFERENCES

[1] P. Comba, M. Kerscher, M. Merz, V. Müller, H. Pritzkow, R. Remenyi, W. Schiek, Y. Xiong, *Chem.–Eur. J.* **2002**, *8*, 5750.
[2] P. Comba, W. Schiek, *Coord. Chem. Rev.* **2003**, *238–239*, 21.
[3] P. Comba, M. Kerscher, *Cryst. Eng.* **2003**, *6*, 197.
[4] C. Bleiholder, H. Börzel, P. Comba, A. Heydt, M. Kerscher, S. Kuwata, G. Laurenczy, G. A. Lawrance, A. Lienke, B. Martin, M. Merz, B. Nuber, H. Pritzkow, *Inorg. Chem.*, accepted.
[5] H. Börzel, P. Comba, H. Pritzkow, *J. Chem. Soc., Chem. Commun.* **2001**, 97.
[6] H. Börzel, P. Comba, K. S. Hagen, M. Kerscher, H. Pritzkow, M. Schatz, S. Schindler, O. Walter, *Inorg. Chem.* **2002**, *41*, 5440.
[7] P. Comba, M. Merz, H. Pritzkow, *Eur. J. Inorg. Chem.* **2003**, 1711.
[8] M. Bukowski, P. Comba, C. Limberg, M. Merz, L. Que Jr., T. Wistuba, *Angew. Chem.* **2004**, *116*, 1303.
[9] P. Comba, M. Kerscher, A. Roodt, *Eur. J. Inorg. Chem.* **2004**, 4640.
[10] P. Comba, A. Lienke, *Inorg. Chem.* **2001**, *40*, 5206.
[11] C. Mannich, P. Mohs, *Chem. Ber.* **1930**, *63*, 608.
[12] C. Mannich, F. Veit, *Chem. Ber.* **1935**, *68*, 506.
[13] A. Samhammer, U. Holzgrabe, R. Haller, *Arch. Pharm.* **1989**, *322*, 551.
[14] U. Holzgrabe, E. Ericyas, *Arch. Pharm.* **1992**, *325*, 657.
[15] G. D. Hosken, C. C. Allan, J. C. A. Boeyens, R. D. Hancock, *J. Chem. Soc., Dalton Trans.* **1995**, 3705.
[16] H. Stetter, K. Dieminger, *Chem. Ber.* **1959**, *92*, 2658.
[17] D. S. C. Black, G. B. Deacon, M. Rose, *Tetrahedron* **1995**, *51*, 2055.
[18] A. N. Cheklov, *Zh. Strukt. Khim.* **2000**, *41*, 359.
[19] H. Börzel, P. Comba, C. Katsichtis, W. Kiefer, A. Lienke, V. Nagel, H. Pritzkow, *Chem.–Eur. J.* **1999**, *5*, 1716.
[20] H. Börzel, P. Comba, K. S. Hagen, M. Merz, Y. D. Lampeka, A. Lienke, G. Linti, H. Pritzkow, L. V. Tsymbal, *Inorg. Chim. Acta* **2002**, *337*, 407.
[21] P. Comba, A. Hauser, M. Kerscher, H. Pritzkow, *Angew. Chem.* **2003**, *115*, 4675.
[22] P. Comba, B. Martin, A. Prikhod'ko, H. Pritzkow, H. Rohwer, *C. R. Chim.*, in press.
[23] H. Börzel, P. Comba, K. S. Hagen, C. Katsichtis, H. Pritzkow, *Chem.–Eur. J.* **2000**, *6*, 914.
[24] R. Caujolle, P. Castera, A. Lattes, *Bull. Soc. Chim. Fr.* **1984**, II-413.
[25] T. Siener, U. Holzgrabe, S. Drosihn, W. Brandt, *J. Chem. Soc., Perkin Trans. 2* **1999**, 1827.
[26] P. Comba, B. Nuber, A. Ramlow, *J. Chem. Soc., Dalton Trans.* **1997**, 347.
[27] P. Comba, M. Kerscher, H. Pritzkow, in preparation.
[28] B. N. Figgis, M. A. Hitchman, 'Ligand Field Theory, its Applications', Wiley-VCH, Weinheim, New York, 2000, p. 154.
[29] P. Comba, R. Ferrari, S. Kuwata, G. A. Lawrance, in preparation.
[30] H. A. Goodwin, F. Lions, *J. Am. Chem. Soc.* **1959**, *81*, 6415.
[31] O. Fuentes, W. W. Pandler, *J. Org. Chem.* **1975**, *40*, 1210.
[32] D. Wang, G. R. Hanson, *J. Magn. Reson. A* **1995**, *117*, 1.
[33] D. Wang, G. R. Hanson, *Appl. Magn. Reson.* **1996**, *11*, 401.
[34] G. M. Sheldrick, 'SHELXTL NT V5.10', Bruker AXS, Madison, Wisconsin, USA, 1999.
[35] P. v. d. Sluis, A. L. Spek, *Acta Crystallogr., Sect. A* **1990**, *46*, 194.
[36] C. K. Johnson, in 'ORTEP: A Thermal Ellipsoid Plotting Program', Oak National Laboratories, Oak Ridge, TN, 1965.

Received November 11, 2004